Electronic structure of boron-doped carbon nanotubes

Takashi Koretsune and Susumu Saito
Department of Physics, Tokyo Institute of Technology, 2-12-1 Oh-okayama, Meguro-ku, Tokyo 152-8551, Japan
(Received 23 November 2007; revised manuscript received 21 March 2008; published 15 April 2008)

We study boron-doped single-walled carbon nanotubes by using first-principles methods based on the density functional theory. The total energy, band structure, and density of states are calculated. From the formation energy of boron-doped nanotubes with different diameters, it is found that a narrower tube needs a smaller energy cost to substitute a carbon atom with a boron atom. By using the result of different doping rates in the (10,0) tube, we extrapolate the result to low boron density limit and find that the ionization energy of the acceptor impurity level should be approximately 0.2 eV. Furthermore, we discuss the doping rate dependence of the density of states at the Fermi level, which is important to realize superconductivity.

DOI: 10.1103/PhysRevB.77.165417 PACS number(s): 73.63.Fg, 73.20.Hb, 68.55.Ln

I. INTRODUCTION

In carbon materials, it has been attempted to dope carriers in order to achieve high transition-temperature superconductivity because of their high Debye frequency. In fact, several studies show superconductivity in carbon materials, such as graphite[1,2] and fullerene[3,4] compounds. In these cases, the carrier is introduced by alkali-metal and/or alkaline-earth-metal doping (intercalation). Hole doping into carbon materials also attracted attention. Substitutional boron doping into fullerenes was theoretically discussed,[5] although the production of a macroscopic amount of B-doped fullerenes has not been reported so far. The recent discovery of superconductivity in boron-doped diamond,[6] therefore, has renewed attention on boron doping.

Among various carbon materials, the carbon nanotube is one of the most important and promising carbon allotropes because of its wide variety in diameter and chirality as well as nanoscale one-dimensional geometry. Because of its dimensionality, there are divergences in the density of states (DOS) at the van Hove singularities, which may invoke interesting phenomena, including superconductivity. So far, superconductivity in carbon nanotubes has been reported in various situations,[7–10] while the mechanism of superconductivity has not been clarified yet. The possibility of boron doping in a superconducting nanotube sample was also discussed.[11] Thus, it is important to examine the carrier doping effect and the possibility of superconductivity in a boron-doped carbon nanotube.

Another important aspect of boron doping into a carbon nanotube is the impurity doping into a semiconducting nanotube. Since the carbon nanotube is considered a new material of nanotechnology, the effect of impurities should be clarified in detail in applications of the nanodevice. As a matter of fact, effects of boron doping in carbon nanotubes were experimentally[12–14] and theoretically[15,16] studied by several groups. As in diamond, boron should make a shallow impurity level in semiconducting tubes in contrast to the substitutional nitrogen impurity.[15] It has been reported that a single-walled or multiwalled carbon nanotube becomes a *p*-type semiconductor by boron doping. In experiment, however, even the amount of doped boron has not been clarified.

In this paper, we study the boron-doped single-walled carbon nanotube (SWCNT) by using the density functional theory to explore the basic properties of boron doping. For this purpose, we perform two types of calculations: diameter dependences and doping rate dependences. Changing the diameter of zigzag and armchair nanotubes, we calculate the formation energy of a B-doped SWCNT and clarify which kind of tubes is favorable for boron doping. We also compute the doping rate dependence of band structure and density of states in a (10,0) tube. We demonstrate that the extrapolation to low boron density limit can indicate the ionization energy of the acceptor impurity level. We also discuss the possibility of superconductivity by using the density of states at the Fermi level $D(\epsilon_F)$.

The paper is organized as follows: In Sec. II, we describe the materials studied and computational method used in this study. In Sec. III, we present the numerical results of optimized structure, total energy, electronic band structure, and density of states. The numerical results and their implications are discussed in Sec. IV. We conclude with a brief summary in Sec. V.

II. SYSTEMS STUDIED AND COMPUTATIONAL METHODS

In the present work, we first focus on zigzag nanotubes, $(m,0)$ with $m=4-12$, and armchair nanotubes, (m,m) with $m=4$, 5, and 6, in order to study the diameter dependence of a B-doped SWCNT. Each tube originally has $4m$ carbon atoms in the unit cell and we substitute one carbon atom with a boron atom in the unit cell, as shown in Fig. 1. To clarify the doping rate dependence, we also study the cases of a larger unit cell for a (10,0) tube, BC_{79} and BC_{119}, and two boron-atom doping B_2C_{78}, wherein boron atoms are placed so that each B-B distance is maximized. Electronic-structure calculations are performed by using a hexagonal supercell so that the interwall distance between tubes is at least 7 Å, which should be large enough to neglect the intertube interactions.

All of the calculations are carried out within the local-density approximation (LDA) in the framework of the density functional theory. We use norm-conserving pseudopotentials,[17,18] the Ceperley-Alder exchange-correlation energy functional[19] that was parametrized by Perdew and Zunger,[20] and a plane-wave basis with a cutoff energy of 50

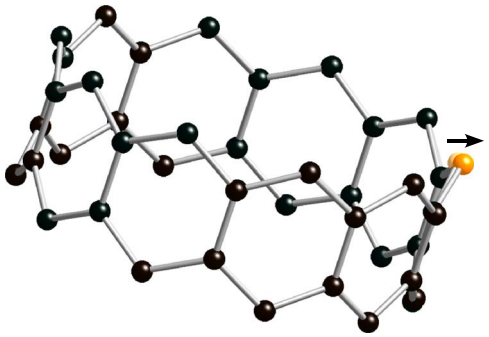

FIG. 1. (Color online) Optimized structure of a boron-doped (10,0) carbon nanotube. There are 39 carbon atoms and 1 boron atom in the unit cell (BC_{39}). The doped boron atom moves outward via geometry optimization as illustrated by the arrow.

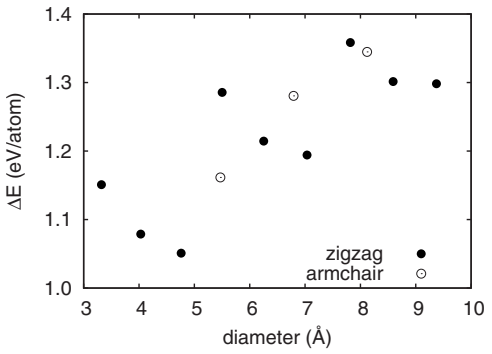

FIG. 2. ΔE defined in Eq. (1) as a function of nanotube diameter. $(m,0)$ zigzag tubes of $m=4-12$ (filled circles) and (m,m) armchair tubes of $m=4$, 5, and 6 (open circles) are plotted.

Ry. Both the geometrical and the electronic degrees of freedom are optimized by a conjugate-gradient method.[21] We take $1\times1\times6$ $\boldsymbol{k}$ points in the first Brillouin zone.

III. RESULTS

A. Optimized geometry and total energy

We first show the result of the geometry and the total energy. Figure 1 illustrates the optimized structure of a boron-doped (10,0) carbon nanotube. Since the boron atom has a larger atomic radius than the carbon atom,[22] the boron atom in the optimized structure locates outside of the original atomic position in the pristine nanotube to stretch the B-C bond length. All of the boron-doped tubes in this study show the same tendency. In the case of the (10,0) tube, boron moves outward from its original position by 0.08 Å, while the tube length stretches by only 0.5%, that is, approximately 0.02 Å per unit cell, indicating that the stretch of the B-C bond length mainly gives rise to the change in internal structures including outward movement of boron. Note that this movement of the substitutional B atom is not so large that even if the tube forms a multiwall, structural effects on adjacent layers, which are typically 3.44 Å away,[23] will be almost negligible.

To discuss the stability of a boron-doped SWCNT, we calculate the formation energy of the substitutional B impurity by comparing the total energy to that of a pristine SWCNT as

$$\Delta E = E(\mathrm{BC}_{n-1}) - E(\mathrm{C}_n)\frac{n-1}{n} - E(\mathrm{B}). \qquad (1)$$

Here, $E(\mathrm{C}_n)$ and $E(\mathrm{BC}_{n-1})$ represent the total energies of a pristine and a boron-doped SWCNT, respectively, and $E(\mathrm{B})$ represents the energy per atom in the α boron.[24,25] We studied the α boron by using the same methodologies with the same pseudopotential as used in the present study. The optimized structure that is obtained has a lattice constant and an angle of 4.96 Å and 58.14°, respectively, which are in good agreement with experiment.[24] Figure 2 shows the result of ΔE as a function of diameter for boron-doped $(m,0)$ zigzag tubes, BC_{4m-1}, with $m=4-12$, and (m,m) armchair tubes, BC_{4m-1}, with $m=4$, 5, and 6.

In the case of zigzag tubes, there is a periodicity in energetics that corresponds to the periodicity of the band structure of zigzag tubes; that is, $(m,0)$ tubes with $m=3p$ $(p=1,2,\ldots)$ have a narrow gap while other tubes have a moderate gap.[26] Narrow-gap tubes should have a smaller "work function" than moderate-gap tubes if their Fermi level is at the same depth from the vacuum. Considering that ΔE, the energy cost of B doping, is a sum of the short-range repulsive-energy cost to replace an atom by a larger one and the energy to remove one electron from the system, the latter energy should be substantially smaller in narrow-gap tubes due to the work function difference while the former energy loss would be more or less the same for similar-diameter tubes. Consequently, B doping into narrow-gap tubes needs less energy than that into moderate-gap tubes.

Except for this periodicity, there is a tendency that ΔE increases with the diameter in both zigzag and armchair tubes, indicating that narrower tubes are more favorable for boron doping. This can be understood as follows: If a boron is doped in a graphene layer that is the infinite diameter limit of the SWCNT, to stretch the B-C bonds, carbon atoms should be pushed or the boron atom should move higher or lower from the graphene layer accompanied by symmetry breaking. On the other hand, if a boron atom is doped in SWCNT, to stretch the B-C bonds, the boron atom can move outward from the tube surface without symmetry breaking. When the curvature is large, a slight movement is sufficient to stretch the B-C bonds. Thus, it needs a relatively small energy to substitutionally dope a boron atom into a SWCNT with a large curvature. Note that the formation energy of boron-doped diamond calculated for BC_{15} is around 1.4 eV,[27] which is similar to the formation energy of the boron-doped nanotubes in the present calculation.

B. Electronic structure and doping rate dependence

Next, we show the electronic structure of B-doped SWCNT at different doping rates. Hereafter, we focus on the (10,0) tube, which is a typical semiconducting carbon nanotube with an energy gap of $E_g=0.75$ eV by the present LDA calculation. One or two borons are substitutionally doped in the unit of C_{40}, C_{80}, and C_{120}. The geometry of each system is fully optimized.

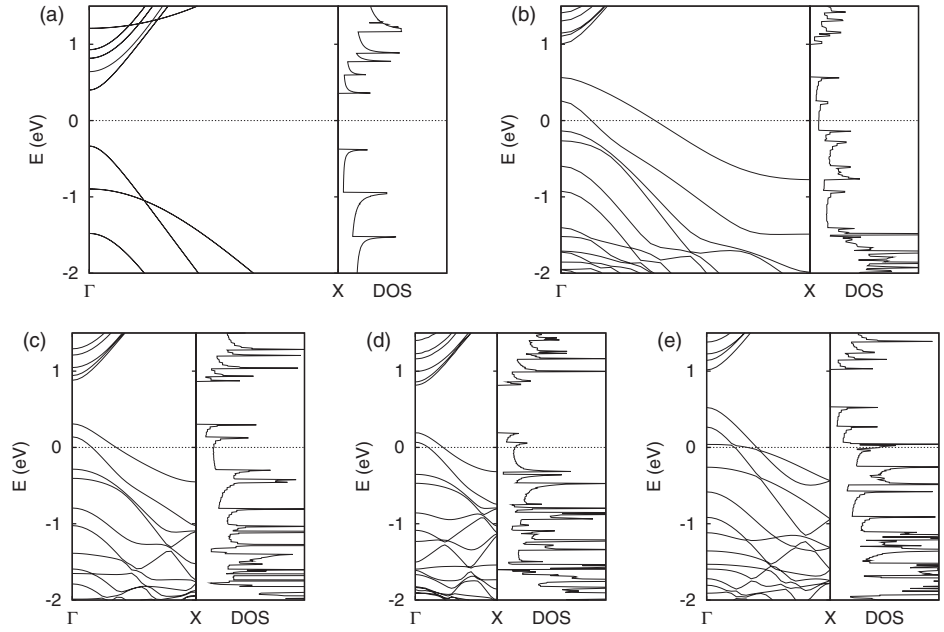

FIG. 3. Band structures and DOSs of pristine and B-doped (10,0) SWCNT: (a) C_{40}, (b) BC_{39}, (c) BC_{79}, (d) BC_{119}, and (e) B_2C_{78}.

Figure 3 shows the electronic band structures and DOSs of C_{40}, BC_{39}, BC_{79}, BC_{119}, and B_2C_{78}. In all of the cases, the highest two bands of the valence band cross the Fermi level. These two bands correspond to the degenerate band of a pristine (10,0) tube, whose degeneracy is lifted by boron doping. It is found that the Fermi level lies below the van Hove singularity at the edge of the valence band. Except for B_2C_{78}, wherein the density of states becomes large because of the third van Hove singularity, $D(\epsilon_F)$ are relatively small and do not change much with the doping rate. The detailed values of $D(\epsilon_F)$, valence-band width, and gap E_g' are summarized in Table I.

IV. DISCUSSION

A. Impurity level

In Sec. III B, we show the doping rate dependence of the electronic structure of a B-doped (10,0) carbon nanotube. Here, we discuss the properties at low boron density limit, that is, the properties of the B impurity level. In the LDA calculation, the bandwidth of the impurity state should go to zero in the infinite impurity distance. In the low B density, the bandwidth of the impurity state will be proportional to the overlap of the impurity state, i.e., $\exp(-L/b)$, where L is the boron-boron distance and b is the characteristic length of the impurity state. At finite densities in the present calculation, however, the bandwidth of the impurity state is still sizable and the impurity band overlaps with the valence band. Thus, the gaps of a B-doped SWCNT in Table I indicate the distance between the top of the impurity band and the bottom of the conduction band. It is noteworthy that the positions of the conduction-band bottom with respect to the valence-band bottom do not change with doping rate in the case of single boron doping, as can be seen from Table I, by summing the valence-band width and the gap energy (20.12–20.19 eV). Therefore, we can assume that the gap between the top of the impurity band and the bottom of the conduction band in the doped tube, $E_g'(L)$, should depend only on the bandwidth of the impurity state as[28]

$$E_g'(L) = E_g'(\infty) + a\,\exp(-L/b), \tag{2}$$

where $E_g'(\infty)$, a, and b are parameters that can be exactly determined from our three doping rate calculations, BC_{39}, BC_{79}, and BC_{119}. The fitted curve is shown in Fig. 4. We find that the gap of the doped tube extrapolates to $E_g'(\infty) = 0.65$ eV. Since the band gap of a pristine (10,0) carbon nanotube is $E_g = 0.75$ eV, there still remains the difference of 0.1 eV between $E_g'(\infty)$ and E_g, which naively corresponds to the ionization energy of the impurity level.

We should care that the ionization energy directly obtained from LDA orbital energies does not necessarily correspond to the ionization energy of the actual impurity level, since the LDA usually underestimates it. For example, the LDA estimates the donor ionization energy in the nitrogen-doped diamond as 0.8 eV,[28] while the experimental value is 1.7 eV. This underestimation is natural because the impurity state is a hydrogenlike state. It is known that the $1s$ Kohn–Sham orbital energy of the H atom in LDA is too shallow, although the LDA total energy is very close to the exact value of −13.6 eV. In fact, by using the same exchange-correlation energy functional as used in this study, the orbital energy of $1s$ state is found to be −6.36 eV. Note that the impurity level can be understood as the hydrogen $1s$ state with effective mass in the medium of the different dielectric constants in the zeroth-order approximation. Thus, it is expected that the ratio of the calculated to the experimental ionization energy of the impurity level corresponds to the ratio of the calculated to the exact ionization energy of $1s$ states, i.e., $6.36/13.6 \sim 0.47$. In fact, in the case of nitrogen-doped diamond, the ratio shows good agreement with that

TABLE I. Electronic structure of a B-doped SWCNT.

	$D(\epsilon_F)$ (1/[atom spin eV])	Valence band width (eV)	Gap (eV)
C_{40}	0	19.37	0.75
BC_{39}	0.020	19.75	0.44
BC_{79}	0.021	19.60	0.57
BC_{119}	0.022	19.53	0.62
B_2C_{78}	0.057	19.57	0.49

for the H atom, i.e., $0.8/1.7 \sim 0.47$. By using this assumption and neglecting the anisotropy of impurity states in the carbon nanotube, we speculate that the ionization energy of the impurity level in the B-doped (10,0) tube is $0.1/0.47 \sim 0.2$ eV.

B. Density of states at the Fermi level

For superconductivity, the density of states at the Fermi level $D(\epsilon_F)$ plays an important role. Thus, the large $D(\epsilon_F)$ in B_2C_{78} is an interesting result. However, considering the fact that BC_{39} and B_2C_{78} have the same boron density, we should control the position of boron atoms as well as the boron density in order to achieve a large density of states. Furthermore, because of experimental difficulty in high-density boron doping,[12,13] a boron concentration of 2.5 at. % seems too large.

To achieve a large $D(\epsilon_F)$ with a low boron concentration, it is promising to use the van Hove singularity at the edge of the valence band. Figure 5 shows $D(\epsilon_F)$ of a B-doped (10,0) carbon nanotube and B-doped diamond[27] as a function of boron density. For comparison, we also plot the density of states of a pristine (10,0) tube regarding the boron concentration as the hole density in the rigid-band picture. For a (10,0) tube, $D(\epsilon_F)$ becomes large with a lowering of the boron concentrations as in the rigid-band picture, which is in sharp contrast with that for boron-doped diamond. From the density of states at the van Hove singularity, we speculate that a boron concentration of $\lesssim 0.4$ at. % is preferable to realize superconductivity. Note that it needs a three dimensionality for superconductivity. Thus, we should consider a bundle of SWCNT or a multiwalled carbon nanotube. Since the present scheme to use the van Hove singularity cannot be applied to a metallic or narrow-gap tube, it might be important to synthesize the bundle of SWCNT or the multiwalled carbon nanotube with each tube being a moderate-gap semiconductor.

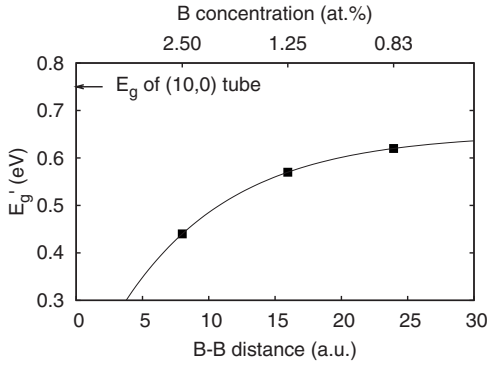

FIG. 4. Gap of a B-doped (10,0) tube as a function of boron-boron distance L. The data are fitted by Eq. (2).

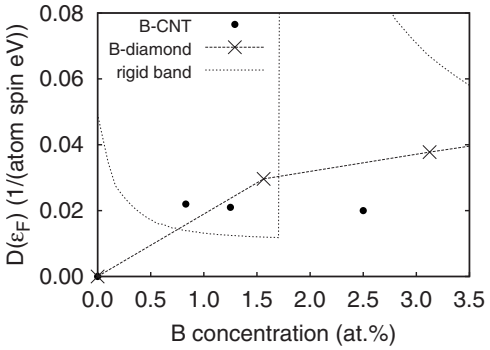

FIG. 5. $D(\epsilon_F)$ of a B-doped (10,0) tube and B-doped diamond. For comparison, we also plot the density of states of a pristine (10,0) tube regarding the boron concentration as the hole density in the rigid-band picture.

V. SUMMARY

We have studied the effect of boron doping in the SWCNT by using LDA calculation. From the result of the geometry optimization and the total energy, it is found that a narrower tube needs a lower energy to exchange a carbon atom with a boron atom. From the result of the doping rate dependence of the band structure and the density of states, we have extrapolated the data to low boron density limit and found that the ionization energy of the B impurity level for a (10,0) tube is about 0.2 eV. We have also studied the density of states at the Fermi level and found that the doping rates in the present study are still too large to realize a high density of states by using the van Hove singularity at the edge of the valence band. We speculate that a lower boron concentration is preferable to realize superconductivity in a boron-doped nanotube, which is in sharp contrast to that of boron-doped diamond.

ACKNOWLEDGMENTS

The authors would like to thank J. Haruyama for useful discussions. The authors would also like to thank A. Oshiyama, T. Nakayama, M. Saito, and O. Sugino for the LDA program used in the present study. Numerical calculations were performed on TSUBAME Grid Cluster at Global Scientific Information and Computing Center of the Tokyo Institute of Technology and SX-7 at Research Center for Computational Science, Okazaki, Japan. This work was partially supported by a Grant-in-Aid for Scientific Research from MEXT, Japan under Contracts No. 19740181, No. 19054005, and No. 18204033, by Asahi Glass Foundation, by Ishikawa Carbon Foundation, and by the 21st Century COE Program by MEXT, Japan through the Nanometer-Scale Quantum Physics Project of the Tokyo Institute of Technology.

[1] N. B. Hannay, T. H. Geballe, B. T. Matthias, K. Andres, P. Schmidt, and D. MacNair, Phys. Rev. Lett. **14**, 225 (1965).
[2] T. E. Weller, M. Ellerby, S. S. Saxena, R. P. Smith, and N. T. Skipper, Nat. Phys. **1**, 39 (2005).
[3] A. F. Hebard, M. J. Rosseinsky, R. C. Haddon, D. W. Murphy, S. H. Glarum, T. T. M. Palstra, A. P. Ramirez, and A. R. Kortan, Nature (London) **350**, 600 (1991).
[4] K. Tanigaki, T. W. Ebbesen, S. Saito, J. Mizuki, J. S. Tsai, Y. Kubo, and S. Kuroshima, Nature (London) **352**, 222 (1991).
[5] Y. Miyamoto, N. Hamada, A. Oshiyama, and S. Saito, Phys. Rev. B **46**, 1749 (1992).
[6] E. Ekimov, V. Sidorov, E. Bauer, N. Mel'nik, N. Curro, J. Thompson, and S. Stishov, Nature (London) **428**, 542 (2004).
[7] M. Kociak, A. Y. Kasumov, S. Guéron, B. Reulet, I. I. Khodos, Y. B. Gorbatov, V. T. Volkov, L. Vaccarini, and H. Bouchiat, Phys. Rev. Lett. **86**, 2416 (2001).
[8] Z. K. Tang, L. Zhang, N. Wang, X. X. Zhang, G. H. Wen, G. D. Li, J. N. Wang, C. T. Chan, and P. Sheng, Science **292**, 2462 (2001).
[9] M. Ferrier, F. Ladieu, M. Ocio, B. Sacépé, T. Vaugien, V. Pichot, P. Launois, and H. Bouchiat, Phys. Rev. B **73**, 094520 (2006).
[10] I. Takesue, J. Haruyama, N. Kobayashi, S. Chiashi, S. Maruyama, T. Sugai, and H. Shinohara, Phys. Rev. Lett. **96**, 057001 (2006).
[11] N. Murata, J. Haruyama, Y. Ueda, M. Matsudaira, H. Karino, Y. Yagi, E. Einarsson, S. Chiashi, S. Maruyama, T. Sugai, N. Kishi, and H. Shinohara, Phys. Rev. B **76**, 245424 (2007).
[12] K. McGuire, N. Gothard, P. L. Gai, M. S. Dresselhaus, G. Sumanasekera, and A. M. Rao, Carbon **43**, 219 (2005).
[13] S. Numao, S. Bandow, and S. Iijima, J. Phys. Chem. C **111**, 4543 (2007).
[14] S. Bandow, S. Numao, and S. Iijima, J. Phys. Chem. C **111**, 11763 (2007).
[15] J. Y. Yi and J. Bernholc, Phys. Rev. B **47**, 1708 (1993).
[16] H. J. Choi, J. Ihm, S. G. Louie, and M. L. Cohen, Phys. Rev. Lett. **84**, 2917 (2000).
[17] N. Troullier and J. L. Martins, Phys. Rev. B **43**, 1993 (1991).
[18] L. Kleinman and D. M. Bylander, Phys. Rev. Lett. **48**, 1425 (1982).
[19] D. M. Ceperley and B. J. Alder, Phys. Rev. Lett. **45**, 566 (1980).
[20] J. P. Perdew and A. Zunger, Phys. Rev. B **23**, 5048 (1981).
[21] O. Sugino and A. Oshiyama, Phys. Rev. Lett. **68**, 1858 (1992).
[22] According to Slater, for example, the empirical atomic radii of boron and carbon are 0.85 and 0.70 Å, respectively [J. C. Slater, J. Chem. Phys. **41**, 3199 (1964)].
[23] Y. Saito, T. Yoshikawa, S. Bandow, M. Tomita, and T. Hayashi, Phys. Rev. B **48**, 1907 (1993).
[24] B. F. Decker and J. S. Kasper, Acta Crystallogr. **12**, 503 (1959).
[25] It is known that the boron atom forms a β-boron structure in the ground state. However, the total energy calculation using LDA predicts almost the same energy in α-boron and β-boron structures [A. Masago, K. Shirai, and H. Katayama-Yoshida, Phys. Rev. B **73**, 104102 (2006)].
[26] N. Hamada, S. I. Sawada, and A. Oshiyama, Phys. Rev. Lett. **68**, 1579 (1992).
[27] S. Saito, T. Maeda, and T. Miyake, in *Diamond Electronics—Fundamentals to Applications*, MRS Symposia Proceedings No. 956, edited by P. Bergonzo, R. Gat, R. B. Jackman, and C. E. Nebel (Materials Research Society, Warrendale, PA, 2007), pp. J14–J03.
[28] S. C. Erwin and W. E. Pickett, Phys. Rev. B **42**, 11056 (1990).